Available online at www.sciencedirect.com
ScienceDirect
Journal of the European Ceramic Society 31 (2011) 1277–1283
www.elsevier.com/locate/jeurceramsoc

Phase relation studies in the CeO_2–La_2O_3 system at 1100–1500 °C

E.R. Andrievskaya [a,*], O.A. Kornienko [a], A.V. Sameljuk [a], A. Sayir [b]

[a] *Frantsevich Institute for Materials Science Problems NAS, Kiev, Ukraine*
[b] *NASA John H. Glenn Research Center, Cleveland, OH, USA*

Available online 22 June 2010

Abstract

Materials based on CeO_2–La_2O_3 system are promising candidates for a wide range of applications, but the phase relationship has not been studied systematically previously. To address this challenge, the subsection of the phase diagram for 1100 and 1500 °C have been elucidated. Samples of different compositions have been prepared from nitrate acid solutions using conventional ceramic techniques; evaporation, drying, and calcinations. The phase relations in the binary CeO_2–La_2O_3 system at 1100–1500 °C were studied from the heat treated samples using X-ray diffraction analysis, petrographic investigation and scanning electron microscopy in the overall concentration range. It was established that in the binary CeO_2–La_2O_3 system there exist fields of solid solutions based on hexagonal (A) modification of La_2O_3, and cubic modification of CeO_2 with fluorite-type structure (F). The systematic study that covered whole composition range excluded formation of new phases. The refined lattice parameter of the unit cell and the boundaries of the homogeneity fields for solid solutions were determined.
© 2010 Elsevier Ltd. All rights reserved.

Keywords: Phase equilibria; Ceria; Lanthana; Solid solutions; Lattice parameters

1. Introduction

Study of phase equilibria in the binary CeO_2–Ln_2O_3 systems is important to advance our understanding of materials compatibility at high temperatures and thus move science forward. The phase diagrams of these systems are considered to be pathways for creation of new materials for a wide range of applications; solid electrolytes in fuel cells, oxygen sensors, catalyst carriers, refractory for furnaces, and thermal barrier coatings. Materials based on ceria, and rare-earth oxides also have applications in medicine, energy production and structural components of heavy machinery due to their unique combination of properties.[1–18]

Solid solutions based on ceria represent the most viable electrolytes operating at moderate temperatures because of their ionic conductivity and high sensitivity to oxygen partial pressure and higher ionic conductivity than in yttria-stabilized zirconia (YSZ) solid solutions. The substitution of Ce^{4+} by suitable trivalent cations such as La^{3+}, Sm^{3+}, Gd^{3+}, Eu^{3+}, Y^{3+} enhances the chemical stability, increases the ionic conductivity and suppresses the reducibility of ceria-based materials.[11] Doping of ceria with low-valence ions, such as La^{3+} and Y^{3+}, is effective to suppress an undesirable ion segregation in the phases based on ceria in so called ceramic carriers of catalysts, which must be reliable in the course of long-term exploitation.[1–8]

The thermal barrier coatings with double ceramic layer ceria and yttria-stabilized zirconia (YSZ), or 8YSZ with pyrochlore-type phase $Ln_2Zr_2O_7$ (Ln = rare-earth elements and yttrium) demonstrate high melting temperatures and have no phase transformations in wide temperature ranges.[8] These coatings show low thermal conductivity, demonstrate chemical inertness and have low thermal expansion coefficient mismatch with the metallic substrate. The good adhesion characteristic to metal substrate and their low sintering rates during operation makes these materials highly desirable for thermal barrier coating applications.

In spite of this relevance of CeO_2–La_2O_3 system for wide range of applications, the phase relationship has not been studied systematically.[5–7,11–20] The absence of systematic and reliable information has led to contradictory statements about the stability of the system.[4,21–30] The boundaries of homogeneity fields for the solid solutions of F–CeO_2 and A–La_2O_3 at 1400 °C were established from 0 to 43 mol% and from 100 to 92 mol% La_2O_3, respectively. The A- and F-phases coexist for concentrations 43–92 mol% La_2O_3. In another study, this system was investigated using samples annealed at 1600 °C and the fluorite-type phase was found stable in the concentrations from 0 to 49 mol% La_2O_3 in Ref. [23]. In another study, stability regimes were identified for concentrations from 0 to 52 mol% La_2O_3.[26] At high

* Corresponding author. Tel.: +38044 424 74 35; fax: +38044 424 21 31.
E-mail address: era@ipms.kiev.ua (E.R. Andrievskaya).

0955-2219/$ – see front matter © 2010 Elsevier Ltd. All rights reserved.
doi:10.1016/j.jeurceramsoc.2010.05.024

lanthana content, from 100 to 96 mol% La_2O_3, the hexagonal A-type La_2O_3 was found. The solid solutions of F–CeO_2 and A–La_2O_3 coexist for the 49–96 mol% La_2O_3 concentration. Yet, another study concluded that the boundary of the homogeneity field A–La_2O_3 was determined to be at 82 mol% La_2O_3.[24] The experimental and analytical study[21] showed that the boundaries of the F phase changes from 0 to 54 mol% La_2O_3 and A phase changes from 100 to 94 mol% La_2O_3 (1600 °C).

This short introduction reveals significant holes in our understanding of the CeO_2–Ln_2O_3 systems. In this paper, we present the phase equilibria in the binary system CeO_2–La_2O_3 and concentration dependences of lattice parameters in the whole range of compositions at temperatures 1100 and 1500 °C. Particular emphasis is placed on the solid solutions based on various polymorphs of the phases. The need to refine lattice parameters of the unit cell and to define the boundaries of the homogeneity fields for solid solutions are highlighted in order to improve design and estimate properties of materials.

2. Experimental

Cerium oxide nitrate, $Ce(NO_3)_3{\cdot}6H_2O$, lanthanum oxide, La_2O_3 (all 99.99%) and analytical-grade nitric acid were used as the starting materials. In total 21 compositions in CeO_2–La_2O_3 system were prepared in the present work for experimental analysis. The specimens were prepared in step 5 mol% from nitrate solutions with their subsequent evaporation and decomposition at 1000 °C for 2 h. Powders were pressed at 10 MPa into pellets of 5 mm in diameter and 4 mm in height. To study phase relationships at 1500 °C thermal treatment of as-prepared samples was carried out in two stages: at 1100 C (for 2799 h in air) and then at 1500 °C (for 150 h in air) in the furnaces with heating elements based on Fecral (H23U5T) and Supercanthal ($MoSi_2$), respectively. To study phase equilibria at 1100 °C, the heat treatment of the samples was carried out in air for 12,780 h. The heating rate was 3.5 °C/min.

The phase composition of the samples was investigated by X-ray (DRON-1.5, Burevestnik, Leningrad), petrographic (MIN-8, optical microscope, LOMO, Leningrad), microstructural phase and electron microprobe X-ray (SUPERPROBE-733, JEOL, Japan, Palo Alto, CA) analyses.

X-ray diffraction analysis of the samples was performed by a powder method at room temperature (CuKα radiation). The scanning speed of 1–4° 2θ/min was employed in the 80–15° 2θ range. The effective precision of the measurements was ±0.0002 nm. Lattice parameters were refined by least squares fitting using the LATTIC program. The uncertainty in the lattice parameter of cubic phases was within 0.0004 nm.

The refractive indexes were measured in highly refractive immersion media (sulfur–selenium alloys or solutions of arsenic tri-bromide in methylene iodide) with an accuracy of ±0.02.

Microstructures were examined on polished sections of annealed samples by electron-probe X-ray microanalysis (EPXMA) in backscattered electron (BSE) and secondary electron (SE) modes. Stoichiometric composition was controlled selectively by chemical and X-ray fluorescence spectrum analysis.

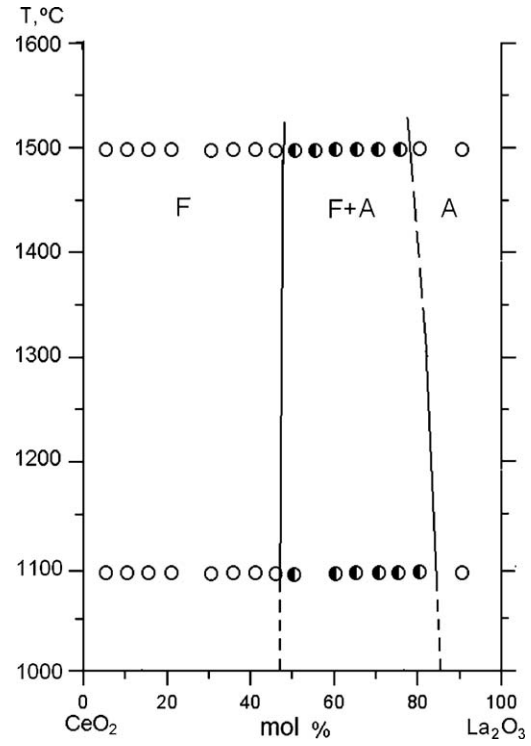

Fig. 1. Phase equilibria in the CeO_2–La_2O_3 system at 1500–1100 °C (◯ – single-phase samples and ◑ – two-phase samples).

3. Results and discussion

The solid-state reaction was investigated between CeO_2 (fluorite-type, F) and La_2O_3 (hexagonal modification of rare-earth oxides, type A) at temperatures 1100 and 1500 °C. The X-ray analysis showed that the CeO_2–La_2O_3 system had two types of solid solutions. The solid solution with cubic symmetry (fluorite F–CeO_2 type) and solid solution hexagonal symmetry (A–La_2O_3 type) coexisted. The phases (A + F) were separated by two-phase field as shown in Fig. 1. The boundaries of the

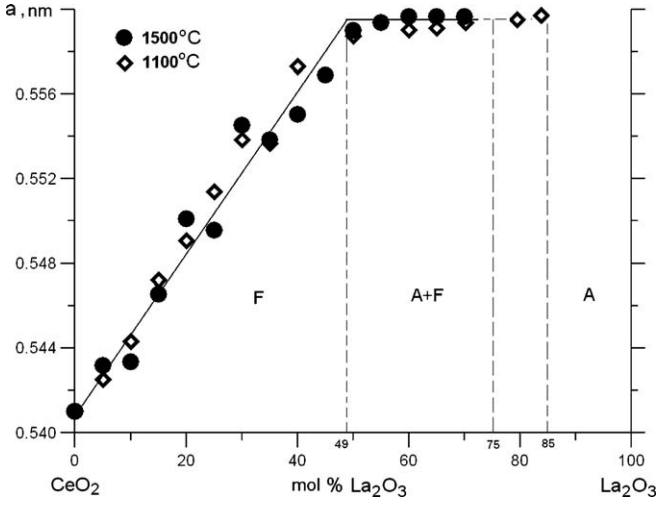

Fig. 2. Concentration dependences of lattice parameters "*a*" of the F-CeO_2 based on solid solutions in the system CeO_2–La_2O_3 heat-treated at 1500 °C (●) and 1100 °C (◊).

Table 1
Phase composition and lattice parameters of the phases in the CeO_2–La_2O_3 system, annealed at 1500 °C for 150 h in air (XRD and petrography data).

Chemical composition (mol%)		Phase composition	Lattice parameters of the phases $a \pm 0.0004$ (nm)			
CeO_2	La_2O_3		⟨F⟩	⟨A⟩		
			a	*a*	*c*	*c/a*
0	100	⟨A⟩*	–	0.6523	0.3855	0.5909
5	95	⟨A⟩*	–	–	–	–
10	90	⟨A⟩*	–	0.6516	0.3828	0.1702
15	85	⟨A⟩*	–	0.6154	0.3828	0.1608
20	80	⟨A⟩*	–	0.6499	0.3847	0.1689
25	75	⟨A⟩** + ⟨F⟩ traces	0.5448	0.6611	0.3828	0.1727
30	70	⟨A⟩** + ⟨F⟩	0.5597	0.6521	0.3843	0.1697
35	65	⟨F⟩ + ⟨A⟩	0.5596	0.3938	0.6068	0.0649
40	60	⟨F⟩↑ + ⟨A⟩↓	0.5597	0.3984	0.5866	0.0679
45	55	⟨F⟩↑ + ⟨A⟩↓	0.5594	–	–	–
50	50	⟨F⟩↑ + ⟨A⟩ traces↓	0.5590	–	–	–
55	45	⟨F⟩	0.5569	–	–	–
60	40	⟨F⟩	0.5550	–	–	–
65	35	⟨F⟩	0.5538	–	–	–
70	30	⟨F⟩	0.5545	–	–	–
75	25	⟨F⟩	0.5495	–	–	–
80	20	⟨F⟩	0.5501	–	–	–
85	15	⟨F⟩	0.5482	–	–	–
90	10	⟨F⟩	0.5433	–	–	–
95	5	⟨F⟩	0.5432	–	–	–
100	0	⟨F⟩	0.5409	–	–	–

Designation of phases: ⟨A⟩ – solid solutions based on hexagonal modification of La_2O_3 and ⟨F⟩ – solid solutions based on cubic modification with fluorite-type structure of CeO_2.
The others designations: basic – phase constituent matrix, ↑ – amount of phase increasing, and ↓ – amount of phase decreasing.
* At given conditions ($T = 1500$ °C for 150 h in air) the hexagonal (A) modification of La_2O_3 unquenchable, and the hexagonal modification of $La(OH)_3$ was observed instead.
** Partial stabilization of A–La_2O_3 was observed.

Table 2
Phase composition and lattice parameters of the phases in the CeO_2–La_2O_3 system, annealed at 1100 °C for 12,780 h in air (XRD data).

Chemical composition (mol%)		Phase composition	Lattice parameters of the phases $a \pm 0.0004$ (nm)			
CeO_2	La_2O_3		⟨F⟩	⟨A⟩		
			a	*a*	*c*	*c/a*
0	100	⟨A⟩*	–	0.6523	0.3855	0.59
5	95	⟨A⟩*	–	–	–	–
10	90	⟨A⟩*	–	–	–	–
15	85	⟨A⟩*	–	–	–	–
20	80	⟨A⟩** + ⟨F⟩ traces	0.5594	0.6492	0.3089	0.48
25	75	⟨A⟩** + ⟨F⟩ traces	0.5594	0.6502	0.3836	0.59
30	70	⟨A⟩** + ⟨F⟩↑	0.5597	0.6462	0.3843	0.59
35	65	⟨F⟩↑ + ⟨A⟩↓	0.5603	0.6468	0.3836	0.59
40	60	⟨F⟩ + ⟨A⟩**↓	0.5603	0.6470	0.3836	0.59
45	55	⟨F⟩↑ + ⟨A⟩**↓	–	–	–	–
50	50	⟨F⟩ + ⟨A⟩**	0.5587	0.6518	0.3821	0.59
55	45	⟨F⟩	–	–	–	–
60	40	⟨F⟩	0.5543	–	–	–
65	35	⟨F⟩	0.5537	–	–	–
70	30	⟨F⟩	0.5538	–	–	–
75	25	⟨F⟩	0.5514	–	–	–
80	20	⟨F⟩	0.5491	–	–	–
85	15	⟨F⟩	0.5472	–	–	–
90	10	⟨F⟩	0.5443	–	–	–
95	5	⟨F⟩	0.5425	–	–	–
100	0	⟨F⟩	0.5409	–	–	–

homogeneity fields for F–CeO_2 and A–La_2O_3 solid solutions (Tables 1 and 2) were determined from samples containing 45–50 mol% La_2O_3 and 75–80 mol% La_2O_3 at 1500 C heat treatment (150 h). Similarly, to determine boundaries of the homogeneity fields for F–CeO_2 and A–La_2O_3 solid solutions we used samples containing 45–50 mol% La_2O_3 and 80–85 mol% La_2O_3 for 1100 °C heat treatment (12,780 h). The lattice parameter as a function of La_2O_3 content is shown in Fig. 2 for the F–CeO_2 solid solution.

The results depicted in Figs. 1 and 2 suggest that the solubility of La_2O_3 in F-modification of CeO_2 is about 49 mol% for both temperatures; 1100 °C and 1500 °C. The lattice parameter of the unit cell of sample containing 50 mol% La_2O_3 increases from a = 0.5409 nm in pure CeO_2 to a = 0.5590 nm for 1500 °C heat treatment while a moderate increase to a = 0.5587 nm was observed for 1100 °C heat treatment. The X-ray diffraction and petrography data have been confirmed by the scanning electron microscopy analysis (Figs. 3 and 4). The microstructure of the

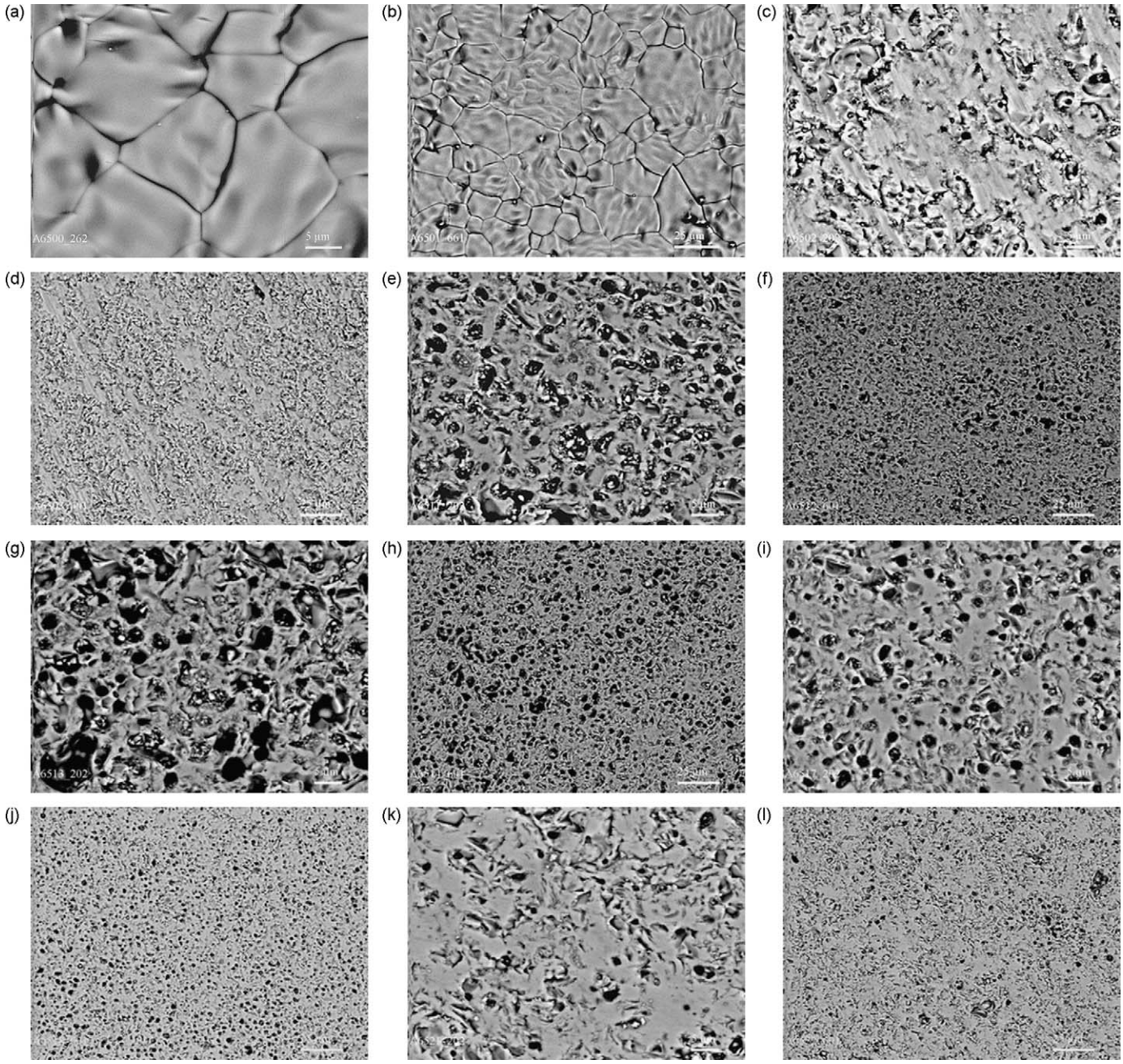

Fig. 3. SEM microstructures of the samples in the CeO_2–La_2O_3 system heat-treated at 1500 °C: (a) ⟨A–La_2O_3⟩ + ⟨F–CeO_2⟩, 50 mol% CeO_2–50 mol% La_2O_3, BSE, ×2000; (b) ⟨A–La_2O_3⟩ + ⟨F–CeO_2⟩, 50 mol% CeO_2–50 mol% La_2O_3, BSE, ×600; (c) ⟨F–CeO_2⟩, 55 mol% CeO_2–45 mol% La_2O_3, BSE, ×2000; (d) ⟨F–CeO_2⟩, 55 mol% CeO_2–45 mol% La_2O_3, BSE, ×600; (e) ⟨F–CeO_2⟩, 75 mol% CeO_2–25 mol% La_2O_3, BSE, ×2000; (f) ⟨F–CeO_2⟩, 75 mol% CeO_2–25 mol% La_2O_3, BSE, ×600; (g) ⟨F–CeO_2⟩, 80 mol% CeO_2–20 mol% La_2O_3, BSE, ×2000; (h) ⟨F–CeO_2⟩, 80 mol% CeO_2–20 mol% La_2O_3, BSE, ×600; (i) ⟨F–CeO_2⟩, 90 mol% CeO_2–10 mol% La_2O_3, BSE, ×2000; (j) ⟨F–CeO_2⟩, 90 mol% CeO_2–10 mol% La_2O_3, BSE, ×600; (k) ⟨F–CeO_2⟩, 100 mol% CeO_2–0 mol% La_2O_3, BSE, ×2000; (l) ⟨F–CeO_2⟩, 100 mol% CeO_2–0 mol% La_2O_3, BSE, ×600; light grains – ⟨F–CeO_2⟩, black – pores.

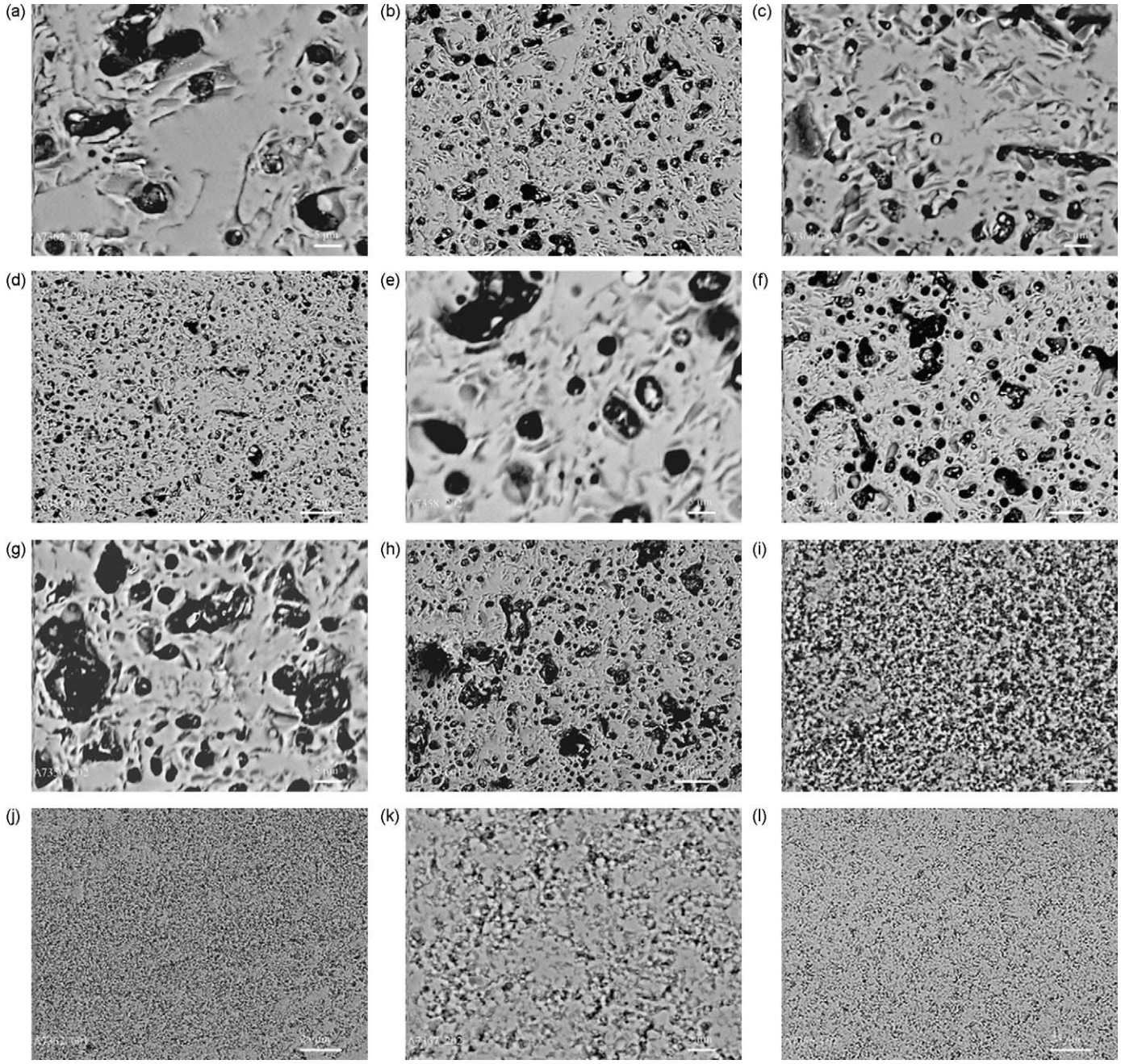

Fig. 4. SEM microstructures of the samples in the CeO_2–La_2O_3 system heat-treated at 1100 °C: (a) ⟨F–CeO_2⟩, 65 mol% CeO_2–35 mol% La_2O_3, BSE, ×2000; (b) ⟨F–CeO_2⟩, 65 mol% CeO_2–35 mol% La_2O_3, BSE, ×600; (c) ⟨F–CeO_2⟩, 70 mol% CeO_2–30 mol% La_2O_3, BSE, ×2000; (d) ⟨F–CeO_2⟩, 70 mol% CeO_2–30 mol% La_2O_3, BSE, ×600; (e) ⟨F–CeO_2⟩, 75 mol% CeO_2–25 mol% La_2O_3, BSE, ×2000; (f) ⟨F–CeO_2⟩, 75 mol% CeO_2–25 mol% La_2O_3, BSE, ×600; (g) ⟨F–CeO_2⟩, 80 mol% CeO_2–20 mol% La_2O_3, BSE, ×2000; (h) ⟨F–CeO_2⟩, 80 mol% CeO_2–20 mol% La_2O_3, BSE, ×600; (i) ⟨F–CeO_2⟩, 90 mol% CeO_2–10 mol% La_2O_3, BSE, ×2000; (j) ⟨F–CeO_2⟩, 90 mol% CeO_2–10 mol% La_2O_3, BSE, ×600; (k) ⟨F–CeO_2⟩, 100 mol% CeO_2–0 mol% La_2O_3, BSE, ×2000; (l) ⟨F–CeO_2⟩, 100 mol% CeO_2–0 mol% La_2O_3, BSE, ×600; light grains – ⟨F–CeO_2⟩, black – pores.

two-phase (A + F) boundary sample with composition 50 mol% CeO_2–50 mol% La_2O_3 shows grains of polyhedral shape, sized in the range from 7.5 to 30 μm (Fig. 3a and b). The dark grey phase (A) exists in small amount in this composition because of its close location to phase boundary and not clearly seen in Fig. 3a due to raised shape of grains. The typical microstructures for the homogeneity field ⟨F–CeO_2⟩ are presented in Figs. 3c-l and 4a-l. It was revealed that the higher the ceria concentration, the smaller are the grains of the F phase (~5.83–0.83 μm), which may be utilized in engineering of high strength material that require small grain size. From the data of electron microprobe and X-ray spectral analysis, the light phase contains cerium only and, therefore, is a solid solution of F–CeO_2. Low sintering activity at given temperatures results in high porosity visible in Figs. 3c-l and 4. The one-phase samples of pure ceria in Fig. 4k look three phase due to pores and surface relief.

The solubility of CeO_2 in hexagonal A–lanthanum oxide reached 25 mol% at 1500 °C heat treated samples and was sign-

ficantly less for 1100 °C heat treated sample; approximately 15 mol% CeO_2. The solid solutions A–La_2O_3 of CeO_2–La_2O_3 system remained stable for both heat treatments; 1500 (150 h) and 1100 °C (12,780 h). When samples containing free La_2O_3 were exposed to a water containing environment (air), they rapidly hydrated. Thus, samples with 70–100 mol% La_2O_3 after 1500 °C heat treatment and samples 50–100 mol% La_2O_3 heat treated at 1100 °C formed hexagonal lanthanum hydroxide upon exposure to air. Increasing of ceria content corresponded to appearance of A-modification of La_2O_3 on X-ray diffraction patterns (Fig. 5). The lattice parameters of the unit cell decreased from a = 0.6523 nm, c = 0.3855 nm for pure $La(OH)_3$ to a = 0.6499 nm, c = 0.3847 nm for 1500 °C heat treated sample. The heat treatment at 100 °C decreased the unit cell parameters to a = 0.6492 nm, c = 0.3089 nm that contained approximately 20 mol% CeO_2.

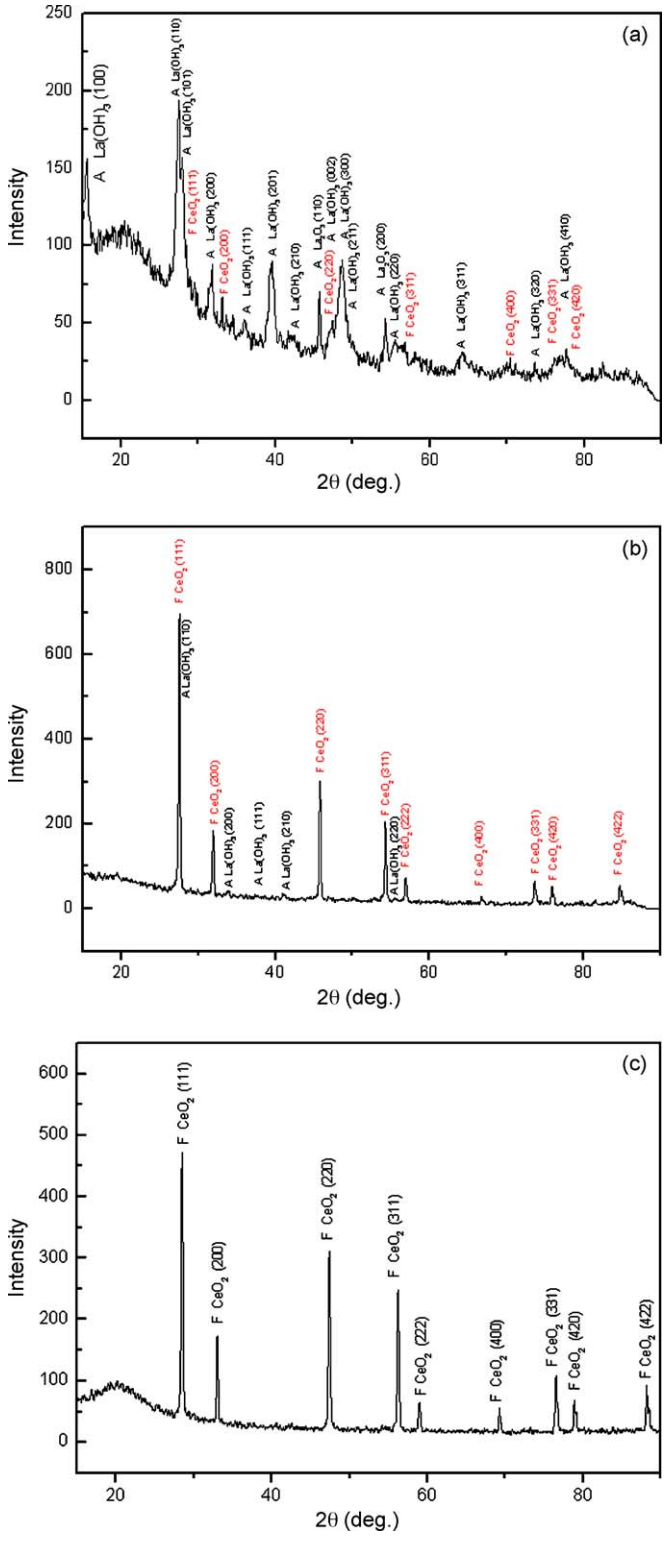

Fig. 5. XRD patterns of the samples for the CeO_2–La_2O_3 system heat-treated at 1500 °C: (a) 20 mol% CeO_2–80 mol% La_2O_3; (b) 50 mol% CeO_2–50 mol% La_2O_3; (c) 100 mol% CeO_2–0 mol% La_2O_3.

4. Conclusions

The phase equilibria in the CeO_2–La_2O_3 system at 1100 and 1500 °C were studied in the whole concentration range. The subsection of the phase diagram has been developed. The solid solutions of hexagonal (A) modification of La_2O_3, and cubic modification of CeO_2 with fluorite-type structure (F) were found that had limited solubility. The fluorite-type structure was stable up to 49 mol% La_2O_3 substitution for the La^{3+} substituted CeO_2 solid solution in spite of much larger La ion size. Only a cubic CeO_2 (Fm3m) phase was identified by XRD analysis in the CeO_2–La_2O_3 system at these temperatures and no evidence of $La_2Ce_2O_7$ pyrochlore phase (Fd3m) was found of the samples annealed at 1100 (12,780 h) and 1500 C (150 h).

Acknowledgments

Dr. E. R. Andrievskaya, Dr. A. V. Sameljuk and Mrs. O. A. Kornienko thank State Funding of Fundamental Research in Ukraine for financial support by the grant SFFR-RFFR No. F28/252-2009; I-7-09.

References

[1]. Ozawa M. Effect of aging temperature on CeO_2 formation in homogeneous precipitation. *J Mater Sci* 2004;**39**:4035–6.
[2]. Kharton VV, Figueiredo FM, Navarro L, Naumovich EN, Kovalevsky AV, Yaremchenko AA, et al. Ceria-based materials for solid oxide fuel cells. *J Mater Sci* 2001;**36**:1105–17.
[3]. Sato K, Yugami H, Hashida T. Effect of rare-earth oxides on fracture properties of ceria ceramics. *J Mater Sci* 2004;**39**:5765–70.
[4]. Mori T, Drennan J, Lee J-H, Li J-G, Ikegami T. Oxide ionic conductivity and microstructures of Sm- or La-doped CeO2-based systems. *Solid State Ionics* 2002;**154–155**:461–6.
[5]. Schmid SK, Pennefather R, Meriani S, Schmid C. Redistribution of Ce and La during processing of Ce(La)–TZP/Al_2O_3 composites. *J Eur Ceram Soc* 1992;**10**:381–92.
[6]. Ivanovskaya MI, Frolova EV, Kotikov DA, Sadykov VA. Features of crystal structure nanoceramics based on CeO2–ZrO2-La2O3. In: *Reports of the first international scientific conference "nanostructural materials"*. 2008. p. 291–2.
[7]. Fan J, Wu X, Yang L, Weng D. The SMSI between supported platinum and CeO_2–ZrO_2–La_2O_3 mixed oxides in oxidative atmosphere. *Catal Today* 2007;**126**:303–12.
[8]. Ma W, Gong S, Li H, Xu H. Novel thermal barrier coatings based on La2Ce2O7/8YSZ double-ceramic-layer systems deposited by electron beam physical vapor deposition. *Surf Coat Technol* 2008;**2022**:2704–8.

[9]. Fan S J., Wu X, Wu X, Liang Q, Ran R, Weng D. Thermal ageing of Pt on low-surface-area CeO_2–ZrO_2–La_2O_3 mixed oxides: effect on the OSC performance. *Appl Catal B: Environ* 2008;**81**:38–48.

[10]. Wei X, Pan W, Cheng L, Li B. Atomistic calculation of association energy in doped ceria. *Solid State Ionics* 2009;**180**:13–7.

[11]. Kumar VP, Reddy YS, Kistaiah P, Prasad G, Vishnuvardhan, Reddy C. Thermal and electrical properties of rare-earth co-doped ceria ceramics. *Mater Chem Phys* 2008;**112**:711–8.

[12]. Wang Y, Guo H, Gong S. Thermal shock resistance and mechanical properties of $La_2Ce_2O_7$ thermal barrier coatings with segmented structure. *Ceram Int* 2009;**35**:2639–44.

[13]. Lopes FWB, de Souza CP, Vieira de Morais AM, Dallas J-P, Gavarri J-R. Determination of RE2Ce2O7 pyrochlore phases from monazite-allanite ores. *Hydrometallurgy* 2009;**97**:167–72.

[14]. Dudek M, Bogusz W, Zych Ł, Trybalska B. Electrical and mechanical properties of CeO_2-based electrolytes in the CeO_2–Sm_2O_3–M_2O_3 (M – La, Y) system. *Solid State Ionics* 2008;**179**:164–7.

[15]. Cutrufello MG, Ferino I, Rombi E, Solinas V, Colón G. Acid-base properties of a ceria-lanthana catalytic system. An adsorption microcalorimetry study. *J Therm Anal Calorim* 2003;**72**:223–9.

[16]. Harrison PG, Kesall A, Wood JV. Chemical microengineering in sol-gel derived fluoride and lanthanide modified ceria materials. *J Sol-Gel Sci Technol* 1998;**13**:1049–55.

[17]. Matsouka V, Konsolakis M, Lambert RM, Yentekakis IV. In situ DRIFTS study of the effect of structure (CeO_2–La_2O_3) and surface (Na) modifiers on the catalytic and surface behavior of Pt/γ–Al_2O_3 catalyst under simulated exhaust conditions. *Appl Catal B: Environ* 2008;**84**:715–22.

[18]. Li J-G, Ikegama T, Mori T, Toshiaki W. Reactive $Ce_{0.8}RE_{0.2}O_{1.9}$ (RE = La, Nd, Sm, Gd, Dy, Y, Ho, Er, and Yb) powders via carbonate coprecipitation. 1. Synthesis and characterization. *Chem Mater* 2001;**13**:2913–20.

[19]. Gerhardt-Anderson R, Nowick AS. Ionic conductivity of CeO_2 with trivalent dopants of different ionic radii. *Solid State Ionics* 1981;**5**:547.

[20]. Butler V, Catlow CRA, Fender BEF, Harding JH. Dopant ion radius and ionic conductivity in cerium dioxide. *Solid State Ionics* 1983;**8**:109.

[21]. Du Y, Yashima M, Koura T, Kakihana M, Yoshimura M. Measurement and calculation of the ZrO_2–La_2O_3–CeO_2 phase diagram. *Calphad* 1996;**20**(1):95–108.

[22]. Brauer G, Gradinger H. Über heterotype Mischphasen bei Seltenerdoxyden. I. *Z Anorg Allg Chem* 1954;**276**:209–26.

[23]. (a) Bevan DJM, Barker WW, Martin RL, Parks TC. Mixed oxides of the type MO_2 (fluorite)–M_2O_3. In: *Proceedings of the fourth conference on rare earth research, vol. 3*. 1964. p. 441;
(b) Bevan DJM, Barker WW, Martin RL, Parks TC. Mixed oxides of the type MO_2 (fluorite)–M_2O_3. In: *Proceedings of the fourth conference on rare earth research, vol. 3*. 1965. p. 441.

[24]. Sibieude F, Hernandez D, Foex M. *CR Acad Sci Ser C* 1974;**278**:1273.

[25]. Bacquet G, Bouysset C, Hernandez D. E.S.R. of Gd^{3+} in La_2O_3 and its solid solutions with CeO_2. *J Phys* 1976;**37**(12):204–7.

[26]. Bevan DJM, Mann AW. The crystal structure of $Y_7O_6F_9$. *Acta Crystallogr* 1975;**B31**:1406–11.

[27]. Minkova N, Aslanian S. Isomorphic substitutions in the CeO_2–La_2O_3 system at 850 °C. *Cryst Res Technol* 1989;**24**:351–4.

[28]. Bae JS, Choo WK, Lee CH. The crystal structure of ionic conductor $La_xCe_{1-x}O_{2-x/2}$. *J Eur Ceram Soc* 2004;**24**:1291–4.

[29]. Morris BC, Flavell WR, Mackrodt WC, Morris MA. Lattice parameter changes in the mixed oxide system $La_xCe_{1-x}O_{2-x/2}$ – a combined experimental and theoretical study. *J Mater Chem* 1993;**3**(10):1007.

[30]. Sibieude F, Schiffmacher G, Caro P. Étude au microscope électronique de structures modulées dans les régions systéme La_2O_3–CeO_2 riches en La_2O_3. *J Solid State Chem* 1978;**23**(3–4):361–7.